Acta Neuropathol (2017) 134:423–440
DOI 10.1007/s00401-017-1745-3

ORIGINAL PAPER

Nogo-A antibodies enhance axonal repair and remyelination in neuro-inflammatory and demyelinating pathology

Benjamin V. Ineichen[1,2,3] · Sandra Kapitza[1,2,3] · Christiane Bleul[1,5] · Nicolas Good[1,2] · Patricia S. Plattner[1,2] · Maryam S. Seyedsadr[1,2,3] · Julia Kaiser[1,2,3] · Marc P. Schneider[1,2] · Björn Zörner[1,2] · Roland Martin[3] · Michael Linnebank[3,4] · Martin E. Schwab[1,2]

Received: 12 January 2017 / Revised: 23 May 2017 / Accepted: 18 June 2017 / Published online: 23 June 2017

Abstract Two hallmarks of chronic multiple sclerosis lesions are the absence of significant spontaneous remyelination and primary as well as secondary neurodegeneration. Both characteristics may be influenced by the presence of inhibitory factors preventing myelin and neuronal repair. We investigated the potential of antibodies against Nogo-A, a well-known inhibitory protein for neuronal growth and plasticity, to enhance neuronal regeneration and remyelination in two animal models of multiple sclerosis. We induced a targeted experimental autoimmune encephalomyelitis (EAE) lesion in the dorsal funiculus of the cervical spinal cord of adult rats resulting in a large drop of skilled forelimb motor functions. We subsequently observed improved recovery of forelimb function after anti-Nogo-A treatment. Anterograde tracing of the corticospinal tract revealed enhanced axonal sprouting and arborisation within the spinal cord gray matter preferentially targeting pre-motor and motor spinal cord laminae on lesion level and above in the anti-Nogo-A-treated animals. An important additional effect of Nogo-A-neutralization was enhanced remyelination observed after lysolecithin-induced demyelination of spinal tracts. Whereas remyelinated fiber numbers in the lesion site were increased several fold, no effect of Nogo-A-inhibition was observed on oligodendrocyte precursor proliferation, migration, or differentiation. Enhancing remyelination and promoting axonal regeneration and plasticity represent important unmet medical needs in multiple sclerosis. Anti-Nogo-A antibodies hold promise as a potential new therapy for multiple sclerosis, in particular during the chronic phase of the disease when neurodegeneration and remyelination failure determine disability evolution.

Keywords Multiple sclerosis · Targeted EAE · Lysolecithin · Remyelination · Nogo-A · Plasticity · Axonal sprouting

Benjamin V. Ineichen and Sandra Kapitza contributed equally and share the first authorship.

Michael Linnebank and Martin E. Schwab contributed equally and share the senior authorship.

✉ Benjamin V. Ineichen
ineichen@protonmail.ch

Martin E. Schwab
schwab@hifo.uzh.ch

1 Brain Research Institute, University of Zurich, Winterthurerstrasse 190, 8057 Zurich, Switzerland

2 Department of Health Sciences and Technology, ETH Zurich, Winterthurerstrasse 190, 8057 Zurich, Switzerland

3 Department of Neurology, University Hospital of Zurich, Zurich, Switzerland

4 Present Address: Department of Neurorehabilitation, School of Medicine, HELIOS Klinik Hagen-Ambrock, Witten/Herdecke University Faculty of Health, Ambrocker Weg 60, 58091 Hagen, Germany

5 Present Address: Translational Genomics Research Institute, Phoenix, AZ, USA

Introduction

Multiple sclerosis is the most common inflammatory disease of the central nervous system (CNS) [40]. In the majority of cases, the disease follows two stages: a first relapsing–remitting disease course followed by a second chronic, progressive phase in which many patients finally become wheelchair bound [53]. Pathogenic hallmarks during early stages are local infiltrations of the CNS tissue by immune cells with subsequent myelin and axonal damage [49, 54, 57]. In the progressive phase, chronic

demyelination and neurodegeneration pre-dominate the pathological picture [30]. Although attempts to repair the damaged myelin are seen, differentiation of oligodendrocyte precursor cells (OPC) among other factors seems to be inhibited, leading to insufficient myelin repair and progressive neurodegeneration [11, 53]. Current therapies address the first, inflammatory phase of multiple sclerosis; however, effective therapies to treat the chronic and progressive stage of the disease are lacking [7, 39].

The adult CNS has an intrinsic capacity for neuronal repair and plasticity after injury which is, however, restricted by growth inhibitory factors such as the membrane protein Nogo-A. This protein is expressed on oligodendrocytes, CNS myelin, and subtypes of neurons [29, 47, 48]. One of its cognate receptors is the Nogo-receptor 1 (NgR1). NgR1 is expressed in OPCs, but not in oligodendrocytes [15]. Nogo-A has other co-receptors besides NgR1 among them being Lingo-1 [34] and sphingosine 1-phosphate receptor 2 (S1PR2) [21]. Importantly, both these molecules have been implicated in myelinogenesis and/or myelin repair (reviewed in [16]).

Blocking Nogo-A or its receptors can promote axonal sprouting, regeneration, and circuit plasticity following CNS injury as shown in different animal models including stroke and spinal cord injury [48]. In the multiple sclerosis animal model of experimental autoimmune encephalomyelitis (EAE), genetic ablation or antibody-mediated neutralization of Nogo-A led to a milder clinical course with smaller lesions (Karnezis et al. 2004) (reviewed by [27]). Studies using vaccination against different epitopes of Nogo-A [9], short interfering RNA to silence Nogo-A [61], or therapeutic application of anti-Nogo-A antibodies [41] confirmed these findings. Nogo-A also seems to play a role in axonal degeneration in EAE and multiple sclerosis [41]. A role of Nogo-A in myelin formation and repair is indicated by the finding that the absence of Nogo-A leads to hypermyelination of node of Ranvier and to highly variable internode length; Nogo-A-deficient mice also showed improved myelin repair after toxic demyelination in the spinal cord using lysolecithin [3].

In multiple sclerosis brain tissue, Nogo-A expression was shown to be upregulated in oligodendrocytes [46], similar to the corresponding findings in EAE mice [51]. Furthermore, albeit Nogo-A antibodies exist in healthy controls as well, younger multiple sclerosis patients and patients with a relapsing disease course showed increased levels of these antibodies in cerebrospinal fluid (CSF) and serum compared to older patients and patients with a chronic-progressive course [43].

The relevance of gene deleted mice for therapeutic translation is limited; we, therefore, addressed two key questions regarding the therapeutic potential of Nogo-A neutralization in multiple sclerosis using function-blocking antibodies: (1) can Nogo-A-neutralization promotes axonal sprouting and regeneration in the spinal cord in EAE? (2) Can inhibition of Nogo-A by antibodies improves remyelination?

Both multiple sclerosis and disseminated EAE are characterized by multiple neuro-inflammatory lesions emerging unpredictably and with a high inter-individual variability all over the CNS. As a consequence, different axonal tracts can be damaged to different extents which render the analysis of axonal regeneration and plasticity extremely challenging if not impossible. We, therefore, chose a model in which a single inflammatory lesion is targeted to a predefined spinal tract system [23]. This targeted EAE model is defined by local infiltration of immune cells (mainly macrophages and CD3 positive T cells) with subsequent demyelination and secondary axonal degeneration. By placing the lesions in the dorsal funiculus at high cervical level, we mainly damaged the corticospinal tract (CST), leading to a strong and long lasting impairment of fine motor skills of the fore and hindlimb. We used lysolecithin-induced demyelination as an additional model to assess the potential Nogo-A antibodies for myelin repair [2]. The injection of lysolecithin only causes minimal axonal damage enabling assessment of remyelination without confounding axonal regeneration [58]. Moreover, this model is characterized by only minimal inflammatory reaction during the de- and remyelination processes [58] except for some macrophages involved in the clearance of myelin debris [25].

Our data demonstrate that the neutralization of Nogo-A by antibodies leads to enhanced recovery of fine motor control of rats after lesioning of the dorsal funiculus of the cervical spinal cord. Anterograde tracing of the CST showed an increased amount of CST sprouting around the inflammatory lesion site. Neutralization of Nogo-A with antibodies also increased the amount of remyelinated axons, thus giving evidence for a dual repair enhancing effect of anti-Nogo-A antibodies.

Materials and methods

Animals

Adult, female Lewis (strain code 004, $n = 35$) and Long Evans rats (LE, strain code 006, $n = 68$; all rats 230–350 g, 3–6 months of age, Janvier, France and Charles River, Italy) were used in this study. Rats from inbred strains are particularly suited for EAE. Therefore, we used Lewis rats for the targeted EAE model. For the lysolecithin experiments, we used rats from the outbred strain LE. The animals were housed in groups of two to four under a constant 12 h light/dark cycle with food and water ad libitum. Animals were handled 2–3 times before doing any interventions with

them. All experimental procedures including animals were approved by the Veterinary Office of the Canton of Zurich, Switzerland (License numbers 53_2012 and 119_2015).

Anaesthesia and post-operative care

For the EAE immunization, rats were anesthetized using 3–5% isoflurane. For all longer-during surgical procedures, anaesthesia was induced by 3–5% isoflurane in the air, followed by a weight-adapted intramuscular injection of a mixture of Domitor® (0.15 mg/kg, Provet), Dormicum® (2 mg/kg, Roche), and Fentanyl25 (0.005 mg/kg, Abbott, USA) for a long-during anaesthesia. At the end of the surgery, sedation and muscle relaxation parts of the anaesthesia were antagonized using weight-adapted subcutaneous injection of a mixture of Antisedan® (0.75 mg/kg, Provet) and Anexate® (0.2 mg/kg, Roche). To minimize post-operative pain and infections, animals received daily subcutaneous injections of Rimadyl® (2.5 mg/kg, Pfizer) and Baytril® (5 mg/kg, Bayer) for consecutive 3–5 days after surgery.

Immunization for targeted EAE lesions

Targeted EAE lesions were induced as previously described [23], with slight adaptations. Briefly, rats were immunized with an emulsion consisting of purified, rat recombinant myelin oligodendrocyte glycoprotein peptide (rrMOG, gift from Doron Merkler, Geneva) corresponding to the N-terminal sequence of rat MOG (amino acids 1–125) in Incomplete Freund's Adjuvant (IFA, Sigma) 1:1. 100 µl of this emulsion was injected subcutaneously at the base of the tail containing an rrMOG dose of 6.25 or 12.5 µg per animal.

Stereotactic surgery to induce targeted EAE and lysolecithin lesions

All injections were made using a 35 gauge cannula (world precision instruments) attached to a Hamilton 10 µl syringe (Hamilton) and injection speed was 10 nl/s. For stereotactic injections, the spinal cord was exposed by a dorsal laminectomy at vertebral level C3. The cannula was left in place for 2 min after injection before withdrawal to avoid reflux.

Targeted EAE

Animals were subjected to a stereotactic injection of a cytokine mixture 18–22 days after immunization. This mixture consisted of recombinant tumor necrosis factor α (TNFα, R&D Systems), recombinant interferon γ (IFNγ, R&D Systems), and recombinant vascular endothelial growth factor (VEGF, R&D Systems, according to [45]), all dissolved in PBS. Four injections were made into segment C3 of the spinal cord: two besides each other in the dorsal funiculus targeting the CST (2 µl each) and two targeting the lateral CST (and rubrospinal tract) in the lateral funiculus (1 µl each). One 2 µl injection contained 250 ng TNFα, 150 U IFNγ, and 500 ng VEGF.

Lysolecithin

The lysolecithin injections were performed as previously described [18], with slight adaptations; briefly, for focal demyelination, 2 µl of 1% lysolecithin (Sigma) were injected targeting the cuneate/gracile fascicle (which contains mainly large caliber axons) on spinal level C3.

Antibody application

The antibody was applied intrathecally via a catheter as previously described [17]. Briefly, a laminectomy at vertebral level L2 was performed and a fine intrathecal catheter (32 gauge, ReCathCo) was inserted into the subarachnoid space and pushed in cranial direction for 30 mm. It was connected to an osmotic minipump (Alzet, model 2ML2, 5 µl/h) which either continuously delivered highly purified mouse monoclonal anti-Nogo-A-antibody 11C7 [38] or control antibodies [anti-cyclosporin (Novartis Pharma Inc.) or anti-BrdU (Serotec)]. Antibody 11C7 has verified in vivo for its Nogo-A blocking ability, whereas the control antibodies do not show in vivo binding [28, 56]. A total of 6 mg antibodies per rat were applied over a period of 14–16 days starting with the day of lysolecithin injection or 3 days after spinal cytokine injection. Control and anti-Nogo-A pumps were randomly assigned to the rats during the operation. Both Nogo-A antibodies and control antibodies were the same antibody type (mouse IgG1). Number-coded animals were randomly mixed in the cages. The pump and catheter were removed after 14–16 days.

Behaviour

The two behavioral paradigms, the irregular horizontal ladder and the Montoya staircase, have been used to assess fine motor fore- and hindlimb recovery of the targeted EAE animals after anti-Nogo-A- or control antibody. Both these tasks highly depend on intact corticospinal and ascending sensory systems of the dorsal funiculus [33, 37]. Animals were habituated and were allowed to train in all setups 4–6 times prior to any baseline recordings. Investigators were blind with regard to the content (anti-Nogo-A or control antibody) of the pumps of the randomly mixed animals in the cages.

The horizontal ladder task is a fine motor skill test to assess fore- and hindlimb function. For this, the animals had to cross a 1 m long irregularly spaced ladder (see Fig. 1b for a schematic). High-speed videos of three

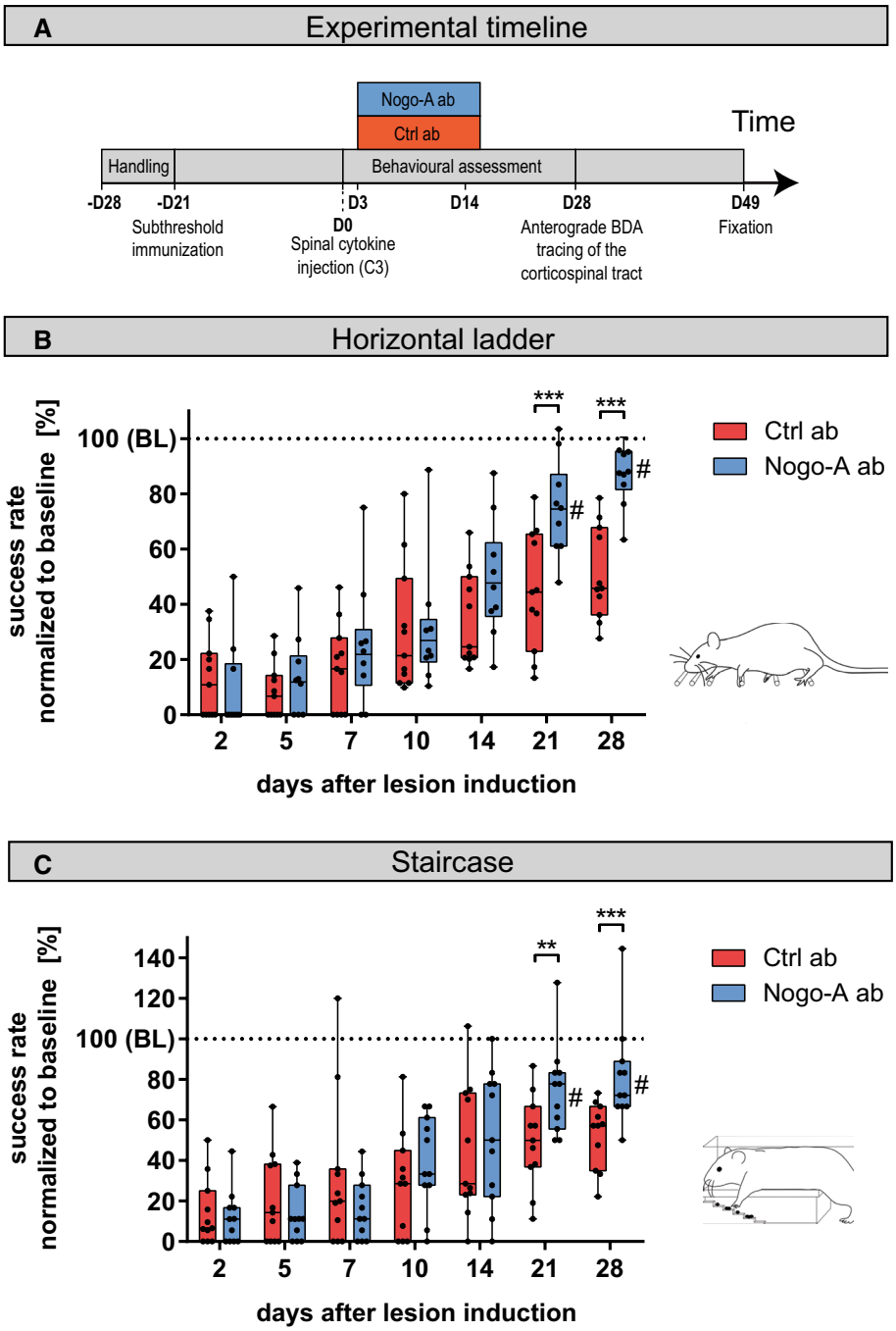

Fig. 1 Functional deficit and subsequent recovery after a neuro-inflammatory dorsal column lesion in anti-Nogo-A and control-antibody-treated rats. **a** Experimental time line; after induction of a neuro-inflammatory lesion at day 0, rats are treated with either anti-Nogo-A- or control antibodies for 2 weeks. Fine motor control of forelimbs was assessed on the irregular horizontal ladder (**b**) and in the staircase pellet grasping task (**c**) up to 4 weeks by determining the percentage of correct steps (ladder) or successfully grasped and eaten sugar pellets (**c**). *Boxplots* show median as horizontal line, upper and lower quartile as box and minimum and maximum as whiskers ($n = 11$ per group). Statistical analysis was done using a two-way ANOVA repeated measure followed by Bonferroni's multiple-comparison test. *Asterisks* indicate significances: $*p < 0.05$, $**p < 0.01$, $***p > 0.001$. #Non-significant compared to baseline. *BL* baseline, *ctrl* control antibody

passages of each animal were analyzed frame-by-frame using the software VirtualDub. Paw slips/misses, improper grasping of rungs, and wrist support were counted as mistakes according to [31]. Total success scores were calculated from the amount of correct steps divided by the total amount of steps.

The staircase test was performed according to [37]. It is a test to assess fine motor skills via skilled reaching for sugar pellets (see Fig. 1c for a schematic). Rats independently use right and left forelimbs to grasp for sugar pellets (45 mg dustless precision pellet, TSE Systems Int. Group) which are presented on both sides on five descending steps with increased reach difficulty. A total amount of 30 pellets were presented at each session lasting 10 min. The success score was calculated from the total amount of retrieved pellets divided by 30.

Anterograde tracing of the corticospinal tract

Anterograde tracing was performed either at the day of targeted EAE lesion induction for axonal sprouting analysis at 3 weeks or at 4 weeks after lesion induction for axonal sprouting analysis 7 weeks after lesion, i.e., after the termination of the behavioural assessments. Animals were mounted to a stereotactic frame and a bilateral craniectomy was performed over the fore- and hindlimb cortices. On each side, seven stereotactic injections of a 10% biotinylated dextran amine (BDA, 10,000 MW, Invitrogen) solution in water were made. Each 450 nl injection was applied at 1 mm depth targeting layer V of the cortex with a 35 gauge cannula attached to 10 µl syringe driven by an electrical pump with a flow rate of 10 nl/s. The coordinates for forelimb were: 1.5 mm anterior/2 mm lateral, 1.5 mm anterior/3 mm lateral, 1 mm anterior/3.5 mm lateral, 1 mm anterior/2.5 mm lateral, and 3.5 mm anterior/1.5 mm lateral, and the coordinates for hindlimb were: 1 mm posterior/2.5 mm lateral and 1.5 mm posterior/2 mm lateral (all coordinates relative to bregma). The cannula remained in place for 2 min after each injection to avoid backflow of the tracer.

Perfusion, tissue preparation, and staining

Immunohistofluorescence/histology

The vascular system of deeply anesthetized animals was flushed via transcardial perfusion using 100 ml Ringer solution containing 100,000 IU/l Heparin (Roche) and 0.25% $NaNO_2$ followed by 300 ml of 4% phosphate-buffered formalin solution (Sigma). Brain and spinal cords were dissected, post-fixed for 4 h, and subsequently transferred to a 30% phosphate-buffered sucrose solution for cryoprotection for at least 3 days. Spinal cords were embedded in TissueTek® O.C.T.™ (TedPella) and frozen in methylbutane (Sigma) to −40 °C. Tissue was coronally cut at 20 or 40 µm on a cryostat (Zeiss) at −20° C. Slices were mounted on objective slides (SuperFrost®) and dried. For immunohistofluorescence, tissue was permeabilized in tris-buffered saline containing 0.3% triton X-100 (Sigma) for 30 min and subsequently incubated overnight at 4 °C with the primary antibody diluted in the same solution containing additionally 4% normal goat serum (Sigma). On the following day, slides were washed in tris-buffered saline containing 0.3% triton X-100 and incubated with the appropriate fluorescently-labelled secondary antibody for 1.5 h at room temperature (1:500, AlexaFluor488 and/or Cy3, Jackson). Some of the sections were counterstained with fluorescent Nissl (1:1000, Invitrogen) or DAPI (1:40,000). The following primary antibodies were used: MBP (1:250, Millipore, AB980), NG2 (1:100, Millipore, AB5320), Olig2 (1:200, Millipore, AB9610), APC (1:300, Millipore, OP80), Iba1 (1:1000, Wako, #019-19741), Ki67 (1:100, Dako, M7240), GFAP (1:500, Wako, Z033429), and DCD16/32 (1:100, BD Bioscience, 553141). EdU staining was performed as previously described [44], with slight adaptations. Briefly, slides with reaction buffer containing Alexa Fluor 555 Azide were incubated at room temperature for 30 min. All slides were then washed in phosphate buffer 30 min, tris 0.05 M 30 min and finally either coverslipped with Mowiol® mounting medium (Calbiochem, for immunohistofluorescence) or dehydrated and coverslipped with Eukitt mounting medium (Sigma, for all non-immune stainings and BDA staining).

Semithin sections and electron microscopy

The perfusion procedure was similar as for the histology except for the fixative: 500 ml of body-tempered modified Karnovsky fixative: 2% formalin, 2.5% glutaraldehyde (Axonlab) in 0.1 M phosphate buffer, and 70 mM calcium chloride (Sigma). Spinal cords with lysolecithin lesions were dissected and post-fixed for 4–10 days in 4% formalin. Tissues were subsequently post-fixed in 1% phosphate-buffered osmium tetroxide (Electron microscopy science) for 4–6 h, dehydrated in ethanol and propyleneoxide (Sigma) and embedded in Epon. Semithin (1 µm) or thin sections (100 nm) were cut on an ultramicrotome (LKB, Austria). The sections were stained with toluidine blue for light microscopy or kept unstained for electron microscopy. Electron microscopic pictures were taken on a Zeiss 10 instrument.

Analysis of anterograde tracing

Mosaic pictures of every eighth BDA-stained spinal cord cross section of segments C1 to C5 were taken at 20× magnification using a slide scanner Axio Scan Z1 (Zeiss). For the analysis of CST fibers which cross the gray–white matter boundary towards the gray matter, a line was placed between the CST and the gray matter using Adobe Illustrator CS6 (Adobe). BDA-positive fibers crossing this line were quantified on every eighth section from C1 to C5 using imageJ (NIH). The center of the neuro-inflammatory lesion at C3 was defined by Nissl staining. For the arborisation analysis of fibers within the gray matter, a grid consisting of 7 vertical and 6 horizontal lines was placed over the right side of the spinal cord gray matter using Adobe Illustrator CS6; this grid was dorsally and laterally adjacent to the dorsal or lateral boundary of the dorsal horn, respectively. Ventrally and medially, it was adjacent to the ventral end of the gray matter or the central canal, respectively. Fibers crossing the horizontal and vertical grid lines were quantified using imageJ. To illustrate the difference

in fiber density between the treatment groups: for each square region in the gray matter (formed by the intersecting horizontal and vertical gridlines), the mean fiber density of control-antibody-treated rats was subtracted from the corresponding mean fiber density of Nogo-A-antibody-treated rats. To plot these data, a heat map was created using Matlab (MathWorks, USA).

Analysis of remyelination using semithin sections/electron microscopy

The amount of disproportionally thin axons compared to the axon diameter was determined within the sensory tracts of the dorsal funiculus consisting mainly of large diameter axons using toluidine blue-stained semithin sections on continuous series of micrographs (at 600×) around the lesion containing the lesion border. Picture series were taken at the level of the lesion center, and approximately 1 mm caudally and 1 mm rostrally of the lesion center. The density of remyelinated axons was related to the corresponding lesion area (expressed as remyelinated axons per 1000 μm^2).

For analysis of remyelination by electron microscopy, G ratios, defined as the diameter of an axon divided by the diameter of the axon plus its associated myelin sheath, were determined. Random images from the lesion were taken (12 electron micrographs per group) at a magnification of 4000× and were quantified by two blinded observers using ImageJ (NIH). A minimum of 100 randomly chosen remyelinated axons per animal were analyzed for G ratio measurements at day 24. In addition, the ratio of demyelinated vs. remyelinated axons was determined in at least ten images at the lysolecithin lesion border per animal (again, at least 100 de- and remyelinated axons were counted).

Analysis of cell counts, OPCs, oligodendrocytes, and optical intensity

All analyzes of optical intensity and cell counts were done in imageJ (NIH). At least three sections per animal were analyzed. All cell counts were normalized to the lesion area. The lysolecithin lesion border was defined using DAPI or Nissl counterstain on the corresponding or adjacent sections; it is defined by a sharp decrease in cell density outside the lesion.

Statistical analysis

All animals were randomly allocated to respective treatment groups and all experimenters were blind to the groups until the end of the statistical analyzes. Data were checked for normal distribution using a Q–Q plot before applying statistics requiring normal distribution. For comparison of behavioural recovery of two treatment groups over time as well as axonal sprouting between treatment groups over different spinal levels, a two-way ANOVA followed by a Bonferroni post hoc correction was done (Figs. 1, 2). Whenever two treatment groups were compared at one timepoint, a two-tailed Student's *t* test with equal variances was performed followed by a Bonferroni post hoc correction, if necessary (Figs. 1, 2, 3, 4, 5, 6). Data from bar plots and data presented in the text part are shown as mean ± standard error of the mean (SEM). Box plots show the median as vertical line, upper/lower quartile as box, and maximal/minimal values as whiskers. Asterisks indicate statistical significance: $*p < 0.05$, $**p < 0.01$, $***p < 0.001$.

Results

Effects of Nogo-A-antibody treatment on functional recovery of fine motor skills after neuro-inflammatory lesion in spinal cord

An experimental timeline is shown in Fig. 1a. After induction of a single neuro-inflammatory lesion in the cervical spinal cord targeting the dorsal funiculus including the CST, both treatment groups, anti-Nogo-A-antibody- and control-antibody-treated animals, showed a strong and comparable drop in fine motor performance on the horizontal ladder and in the staircase grasping task. Performance started to improve around days 10–14 in both groups and plateaued between 21 and 28 days. From day 21 onward, the Nogo-A-antibody-treated group showed a significantly higher recovery compared to control-antibody-treated animals in both tests (Fig. 1b, c).

Lesion size and lesion cell counts between treatment groups 3 weeks after induction of a neuro-inflammatory lesion

EAE lesions targeted to the dorsal funiculus of the spinal cord are defined by a local increase in cell density as shown by Nissl cell body staining and a matching area of demyelination as shown by Eriochrome myelin staining (Fig. 2a–d). The lesion affected the ascending sensory tracts cuneate and gracilis much more than the CST (Fig. 2e), but no significant differences were present between the two antibody treatment groups as shown by Neurolucida 8.0 3D lesion reconstruction. Quantification of cell density within the neuro-inflammatory lesion using Nissl cell body staining or DAPI staining also showed no significant difference between anti-Nogo-A-antibody and control-antibody group (Fig. 2f–k).

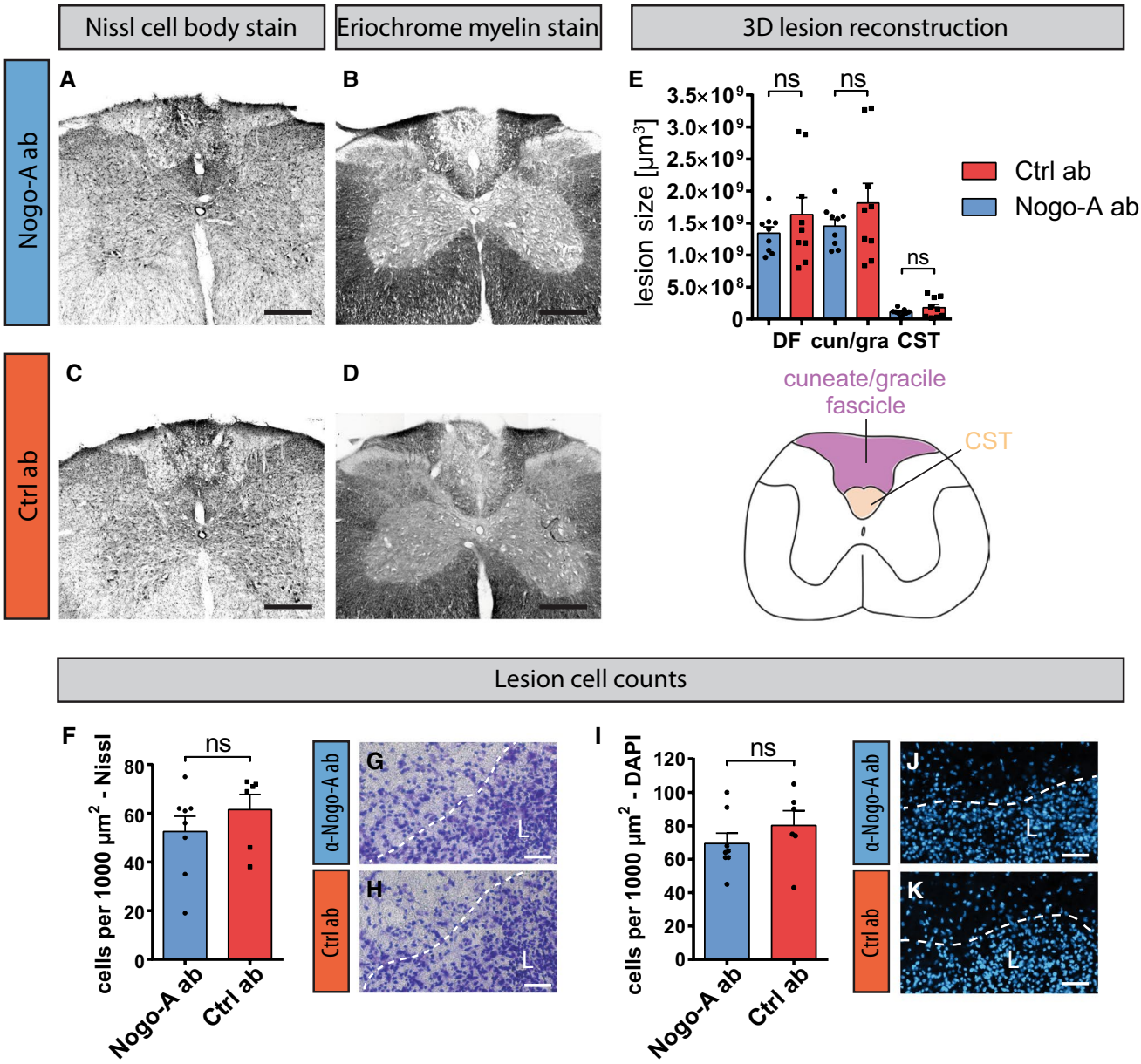

Fig. 2 Lesion size and cell counts in neuro-inflammatory lesions of anti-Nogo-A and control-antibody-treated rats. Targeted EAE lesions appear as cell-dense areas in the Nissl cell body stain (**a**, **c**, **g**, **h**) with matching demyelination in the Eriochrome myelin staining (B, D). No difference was observed in lesion volume in the cuneate/gracile fascicles, the corticospinal tract (CST), or the complete dorsal funiculus between the treatment groups ($n = 9$ per group) as assessed by 3D lesion reconstruction (**e**). No significant differences in density of Nissl-stained nuclei within the lesion between the treatment groups were observed (**g**, **h**, quantification **f**) or DAPI-stained nuclei (**j**, **k**, quantification **i**). The lesion and its border (dashed white line in **g**, **h**, **j**, and **k**) are defined by the high cell density. *Bars* represent mean ± SEM. Statistical analysis was done using a one-way ANOVA in (**e**) and an unpaired, two-tailed, homoscedastic *t* test followed by Bonferroni's multiple-comparison test in (**f**). *Scale bars* **a**–**d** 1 mm, **g**, **h**, **j**, and **k** 40 µm. *CST* corticospinal tract, *cun/gra* cuneate and gracile fascicles; *DF* dorsal funiculus, *ctrl* control antibody, *L* lesion, *ns* non-significant

Sprouting of CST axons at the lesion site

To quantify the sprouting of CST fibers in the vicinity of the lesion site, bilateral anterograde motor cortex BDA tracing was performed and CST fibers leaving the tract and entering the gray matter were quantified (fibers intersecting with the dashed green line in Fig. 3a–c) in the cervical spinal cord from C1 to C5 (lesion center: C3). All fiber counts were normalized to the amount of BDA-labelled axons in the CST on the corresponding spinal levels. Three weeks after induction of the neuro-inflammatory injury, more CST fibers grew into the gray matter in the anti-Nogo-A group

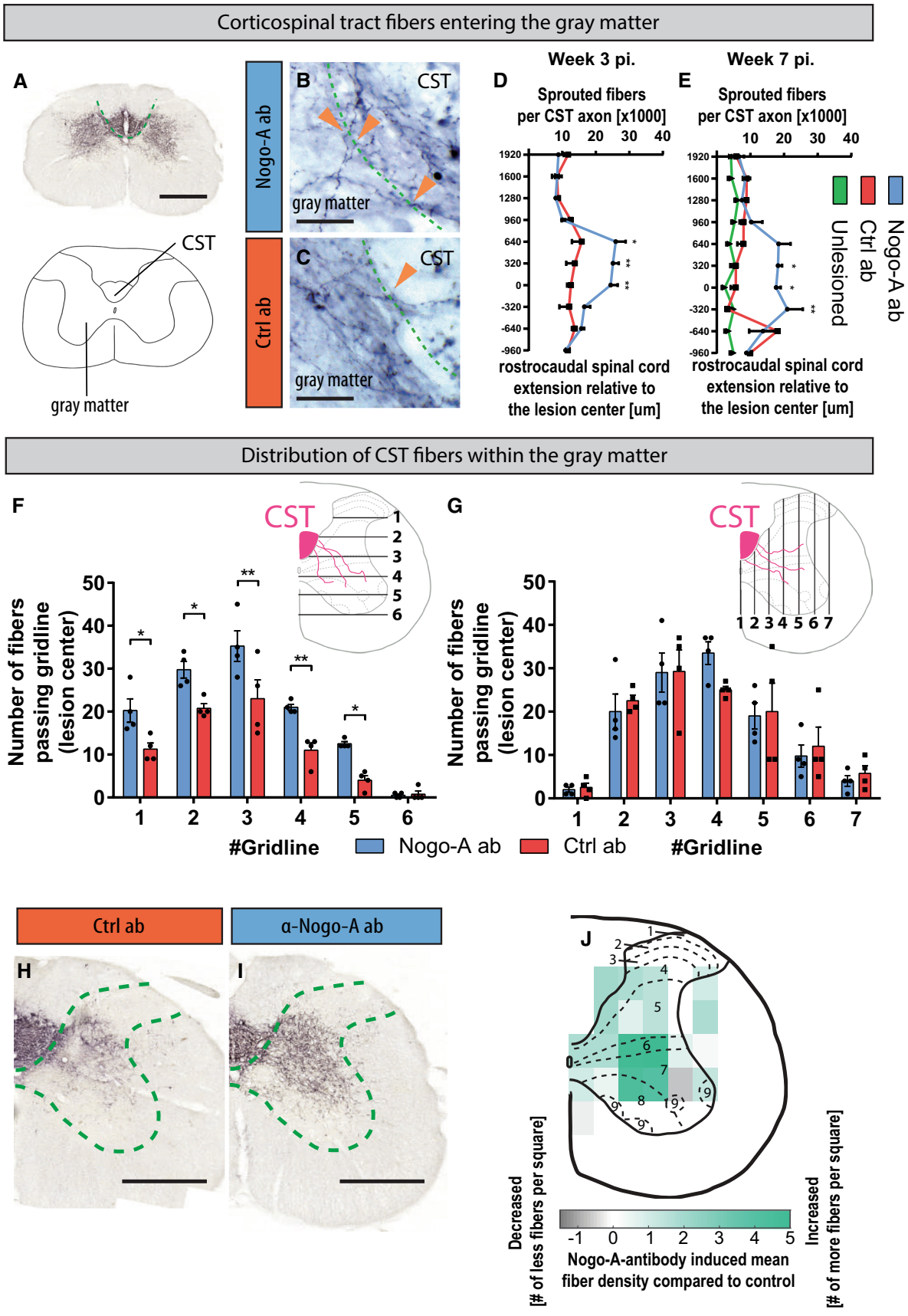
Corticospinal tract fibers entering the gray matter
A
CST
gray matter
Nogo-A ab
Ctrl ab
B
CST
gray matter
C
CST
gray matter
Week 3 pi.
D
Sprouted fibers per CST axon [x1000]
10 20 30 40
1920 1600 1280 960 640 320 0 -320 -640 -960
rostrocaudal spinal cord extension relative to the lesion center [um]
Week 7 pi.
E
Sprouted fibers per CST axon [x1000]
10 20 30 40
1920 1600 1280 960 640 320 0 -320 -640 -960
rostrocaudal spinal cord extension relative to the lesion center [um]
Unlesioned
Ctrl ab
Nogo-A ab
Distribution of CST fibers within the gray matter
F
CST
1 2 3 4 5 6
Number of fibers passing gridline (lesion center)
50 40 30 20 10 0
1 2 3 4 5 6
#Gridline
Nogo-A ab
Ctrl ab
G
CST
1 2 3 4 5 6 7
Number of fibers passing gridline (lesion center)
50 40 30 20 10 0
1 2 3 4 5 6 7
#Gridline
Ctrl ab
α-Nogo-A ab
H
I
J
Decreased [# of less fibers per square]
Increased [# of more fibers per square]
-1 0 1 2 3 4 5
Nogo-A-antibody induced mean fiber density compared to control

◂**Fig. 3** Corticospinal tract (CST) fibers sprouting and branching in the perilesional gray matter is enhanced in the anti-Nogo-A group 7 weeks after neuro-inflammatory lesion. **a–e** Quantification of BDA-stained CST fibers crossing *dashed green line* (*gray–white* matter boundary **a**) on different spinal levels: more fibers enter the *spinal gray matter* in the anti-Nogo-A group, mainly around the lesion center at level C3 at 7 weeks (anti-Nogo-A: **b**, Ctrl antibody: **c**, *green dashed line* represent boundary between CST and *gray matter*, *orange arrowheads* label fibers intersecting with white–gray matter boundary, E quantification, $n = 4$ per group) and 3 weeks after neuro-inflammatory lesion (**d** anti-Nogo-A: $n = 8$, ctrl antibody: $n = 5$). **f–j** Analysis of CST arborisation in gray matter upon anti-Nogo-A treatment suggests a preference of branching in the dorso-ventral (**f**) rather than lateral direction (**g**) targeting mainly the pre-motor spinal cord laminae (ctrl: **h**, anti-Nogo-A: **i**). **j** Heat plot illustrating the mean difference in CST fiber densities between anti-Nogo-A-antibody-treated rats and control-antibody-treated rats 7 weeks after induction of the neuro-inflammatory injury; fibers in the anti-Nogo-A group are increased mainly in the pre-motor laminae (5–8) (*green* indicates increased fiber density, and *gray* indicates decreased fiber density compared to control-antibody-treated rats). *Bars* represent mean ± SEM. Statistical analysis was done using a two-way ANOVA repeated measure followed by Bonferroni's multiple-comparison test. Asterisks indicate significances: $*p < 0.05$, $**p < 0.01$, $***p > 0.001$. *Scale bars*: **a**, **h**, **i** 1 mm; **d**, **e** 50 μm. *CST*, corticospinal tract; ctrl, control antibody; *pi*, post injury

compared to the control-antibody group around the lesion center and rostrally of it at spinal level C3 (Fig. 3d). The majority of these fibers persisted up to 7 weeks (Fig. 3b, c, e). Importantly, no statistical significant difference in the amount of axonal damage between the treatment groups, quantified as the percentage of BDA-positive axons surviving caudally to the lesion, was apparent (Ctrl 67.3 ± 18.7%, anti-Nogo-A 41 ± 11.9% surviving CST fibers caudally to the lesion, *t* test: $p = 0.32$, data not shown).

Effects of anti-Nogo-A antibodies on CST innervation density of gray matter 7 weeks after neuro-inflammatory lesion

Since there was a significant difference in the amount of CST fibers entering the gray matter around the lesion site at 7 weeks after neuro-inflammatory lesion to the cervical spinal cord, we asked whether these fibers show arborisation within the appropriate pre-motor or motor spinal laminae. We determined the CST fiber density by placing an aligned grid over the gray matter and quantified the intersections of the fibers with these gridlines (Fig. 3f, g). The fiber density was different between the two treatment groups: anti-Nogo-A-antibody-treated animals showed higher counts mainly in the intersections with the horizontal lines, indicating a significantly higher degree of branching in the dorso-ventral dimension (Fig. 3f, g). Notably, the enhanced fiber density in the anti-Nogo-A-antibody group seemed to target specifically the pre-motor and motor laminae of the gray matter (laminae 5–8, Fig. 3h, i). The distinct fiber distribution pattern in the gray matter was confirmed by a heat plot showing an increased mean fiber density of the anti-Nogo-A group compared to the control-antibody group in laminae 5–8 (Fig. 3j).

Effects of Nogo-A-antibody treatment on remyelination at 16 and 24 days after induction of a demyelinating lesion

Since the protracted degenerative processes in EAE overlap with myelin repair, this model has limitations in determining specific roles in myelin repair of a given therapy [6]. Therefore, to assess the potential remyelinating effect of anti-Nogo-A antibodies in a pure model of demyelination, we induced such a lesion by lysolecithin injection into the dorsal funiculus of spinal cord at level C3. Another advantage of lysolecithin is that it does only induce minimal axonal damage upon injection [2].

We first investigated a potential effect of anti-Nogo-A- or control antibodies on demyelination. Three days after lysolecithin injection and anti-Nogo-A- or control-antibody treatment, the dorsal funiculus lesions showed complete, focal demyelination with no difference in lesion volumes between the treatment groups (ctrl 0.21 ± 0.14 mm^2, anti-Nogo-A 0.24 ± 0.07 mm^2, *t* test: $p = 0.76$).

The lysolecithin lesion was targeted to the cuneate/gracile fascicle of the dorsal funiculus consisting of large caliber axons. These large caliber axons allow for unequivocal designation of remyelinated axons in semithin sections. Remyelination was assessed by quantifying these large caliber axons with disproportionally thin myelin sheaths [2]. At 3 days after the lesion, very few or no such axons were observable in either group (ctrl 0.85 ± 0.54, anti-Nogo-A 0.66 ± 0.15 thinly myelinated axons per 1000 μm^2, Fig. 4a, d, g). At 16 days, all the groups, also the phosphate-buffered saline (PBS)-treated controls, showed the presence of remyelinated axons; the anti-Nogo-A-antibody-treated group, however, had more than double the number of such axons as compared to the two control groups (ctrl antibody 6.8 ± 2.1, anti-Nogo-A 15.5 ± 3.1, phosphate-buffered saline (PBS) 5.3 ± 0.79 thinly myelinated axons per 1000 μm^2, *t* test: $p = 0.02$, data pooled from three separate experiments, Fig. 4b, e, g).

To address a more clinically relevant setting (in which treatment would only start after lesion emergence), we postponed the antibody treatment for 10 days after lesion induction. In this case, a 2 week anti-Nogo-A-antibody treatment again leads to remyelinated axon numbers more than two times higher than those of the control-antibody group at day 24 after lesion induction (ctrl 14.7 ± 6.3, anti-Nogo-A 34.5 ± 4.4, unlesioned control tissue 43.9 ± 2.3 thinly myelinated axons per 1000 μm^2, *t* test: $p = 0.008$, Fig. 4c, f, g).

Electron microscopic analyzes of 100 remyelinated axons chosen at random at day 24 showed no difference in G ratio (G ratio being a measure of relative myelin sheath thickness compared to the axonal diameter) between Nogo-A-antibody and control-antibody treatment (G ratio ctrl 0.89 ± 0.003, G ratio anti-Nogo-A 0.89 ± 0.004, *t* test: $p = 0.22$, Fig. 4h–k). However, the analysis of de- and remyelinated axons at the lesion border showed a significant difference in the amount of still demyelinated axons between the treatment groups: whereas in the control group, a total of 25% demyelinated axons remained (axons defined by a G ratio of 1), the anti-Nogo-A had about 10% naked axons remaining indicating enhanced myelin repair in the Nogo-A-antibody-treated group (ctrl antibody 24.4 ± 4.0, anti-Nogo-A 9.7 ± 2.0 demyelinated axons at the lesion border, *t* test: $p = 0.03$, Fig. 4h, i, l).

Together, these results show that Nogo-A neutralization enhances remyelination at different timepoints after a demyelinating insult in the adult rat spinal cord white matter.

Effects of Nogo-A-antibody treatment on microglia, macrophages, and astrocytes

To investigate potential mechanisms of the enhanced remyelination induced by the Nogo-A-antibody treatment, we looked at the reaction of glial cells upon Nogo-A-antibody treatment at different timepoints after lysolecithin lesion induction.

We first investigated potential effects of anti-Nogo-A treatment on microglia/macrophages and astrocytes in the lesion, where the remyelination takes place. The lysolecithin lesion border was defined using DAPI counterstain on corresponding or adjacent sections. Macrophages are critically involved in myelin debris clearance and remyelination [26], and it has been shown that macrophages express the Nogo-A receptor NgR1. This Nogo-A receptor has been shown to mediate the efflux of macrophages from inflamed peripheral nerves [13]. We quantified the amount of macrophages in the demyelinated lesions at days 3, 16, and 24 after lysolecithin injection in semithin sections defined as large and debris-filled cells within the lesion [25] (Fig. 5a–c). There was no difference in the amount of these cells at neither timepoint between the treatment groups. To confirm this, we used Iba1 immunostaining for activated microglia/macrophages; abundant Iba1 signal was found at all investigated timepoints within the lesion with a sharp decrease at the lesion border (Fig. 5d–d″, e–e″, images from day 16). No difference in the Iba1 + cell counts between anti-Nogo-A and control-antibody treatment was observed (Fig. 5f). We also quantified CD16/32 positive cells, being a marker for the pro-inflammatory macrophage subtype M1 [36] (Fig. 5g, h); however, we also did not observe a difference in the optical intensity of immune-staining between the treatment groups and timepoints for M1 macrophages (Fig. 5i).

Reactive astrocytes, stained for GFAP, were abundant within the lysolecithin lesion (Fig. 5k–k″, l–l″, images from day 16), and again, no difference in the optical density of the GFAP signal between anti-Nogo-A and control group was observed (Fig. 5j).

Effects of Nogo-A-antibody treatment on proliferation, migration, and differentiation of OPCs

To address a potential effect of Nogo-A-neutralization on distinct steps of oligodendrocyte development, i.e., proliferation or migration of OPCs or differentiation into oligodendrocytes, we looked at OPCs and oligodendrocytes in the lysolecithin lesion using different immunofluorescence stainings. Essential for this experiment is the well-defined and reproducible timeline for demyelination and subsequent myelin repair upon injection of lysolecithin [10, 32]: demyelination peaks at 2–3 day post injection, OPC activation and recruitment at 3–7 days, differentiation of OPCs to oligodendrocytes at 7–10 days, and remyelination is well detectable from day 14 after lesion on. EdU was injected subcutaneously at day 4 after lysolecithin lesion induction (around the peak of OPC proliferation after lysolecithin lesion induction). Animals were sacrificed at 5, 7, and 16 days after lysolecithin injection. An experimental timeline is shown in Fig. 6a.

The amount of labelled OPCs decreases after the injection of EdU until day 16, probably due to repeated cycles of cell proliferation causing a dilution of EdU over time. Therefore, the different timepoints should not be compared for the EdU cell counts. There was no difference in OPC proliferation between the treatment groups at any time, suggesting no effect of the anti-Nogo-A-antibody treatment on OPC proliferation (Olig2/EdU double-positive cells, Fig. 6b, d–d″, e–e″). Similar results were obtained when quantifying NG2/EdU double-positive cells (Fig. 6f).

Effects on migration of OPCs could yet be another potential mechanism by which the Nogo-A immunotherapy could influence remyelination. We counted the Olig2 positive cells within a concentric strip of 50 µm diameter at the lesion border at early timepoints (5 and 7 days) after lesion induction. No difference in the amount of Olig2 positive cells was observed in this region that is critical for myelin repair (Fig. 6c, d–d″, e–e″). Similar results were found for NG2 positive cells at the lesion border (Fig. 6g).

Nogo-A could also be involved in the OPC differentiation towards oligodendrocytes. Indeed, Lingo-1, a membrane protein associated with the Nogo-receptor NgR1, has been shown to be negatively involved in OPC differentiation [35]. The quantification of Olig2/APC

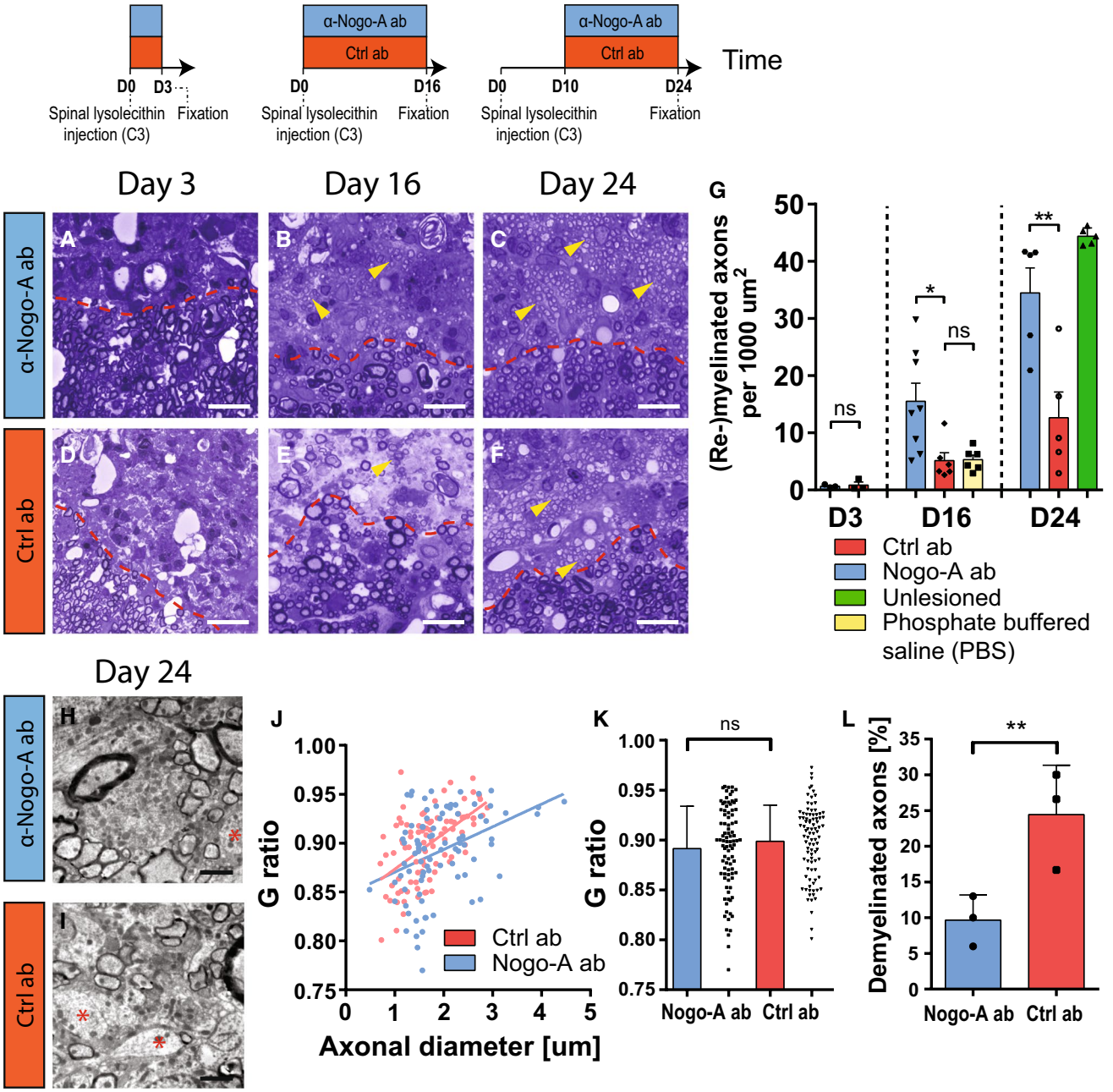

Fig. 4 Remyelination after lysolecithin-induced demyelination in the spinal cord dorsal funiculus upon anti-Nogo-A treatment. Three days after lesion induction in the sensory parts of the dorsal funiculus, only very few or no remyelinated axons (as defined by disproportionally thin myelin) were detectable at the lesion border in all the groups [anti-Nogo-A ($n = 3$) and ctrl group ($n = 3$)] in toluidine blue-stained semithin sections (A, D, quantification in G). Sixteen (anti-Nogo-A: $n = 8$; Ctrl antibody: $n = 6$; phosphate-buffered saline (PBS): $n = 6$; arrowheads label disproportionally thinly myelinated axons representing remyelination) and 24 days (anti-Nogo-A: $n = 6$; ctrl antibody: $n = 6$; unlesioned control tissue: $n = 5$; arrowheads label disproportionally thinly myelinated axons representing remyelination) after induction of the lesion, high numbers of remyelinated fibers were present in the anti-Nogo-A and lower numbers in the control groups (day 16: **b**, **e**; day 24: **c**, **f**; quantification in **g**). These results are confirmed at day 24 using electron microscopy: even though there is no difference in **g** ratio between the treatment groups (representative images **h** and **i**, *red stars* label demyelinated axons; scatter plot quantification with regression *lines* **j**; *bar graphs* showing mean G ratio of groups, $n = 3$ per group), a significant difference in the amount of still demyelinated axons was found (**h**, **i**, and **l**, axons with a G ratio of 1 represent demyelinated axons: about 25% of axons remain demyelinated in the control group compared to 10% in the anti-Nogo-A group, $n = 3$ per group) confirming enhanced remyelination upon Nogo-A-antibody treatment. *Bars* represent mean ± SEM. Statistical analysis was done using unpaired, two-tailed, homoscedastic *t* tests followed by a Bonferroni's multiple-comparison test. *Asterisks* indicate significances: $*p < 0.05$, $**p < 0.01$, $***p > 0.001$. Scale bars: A-F: 12 µm, H, I: 2 µm. Ctrl, control antibody; m, macrophage; ns, non-significant

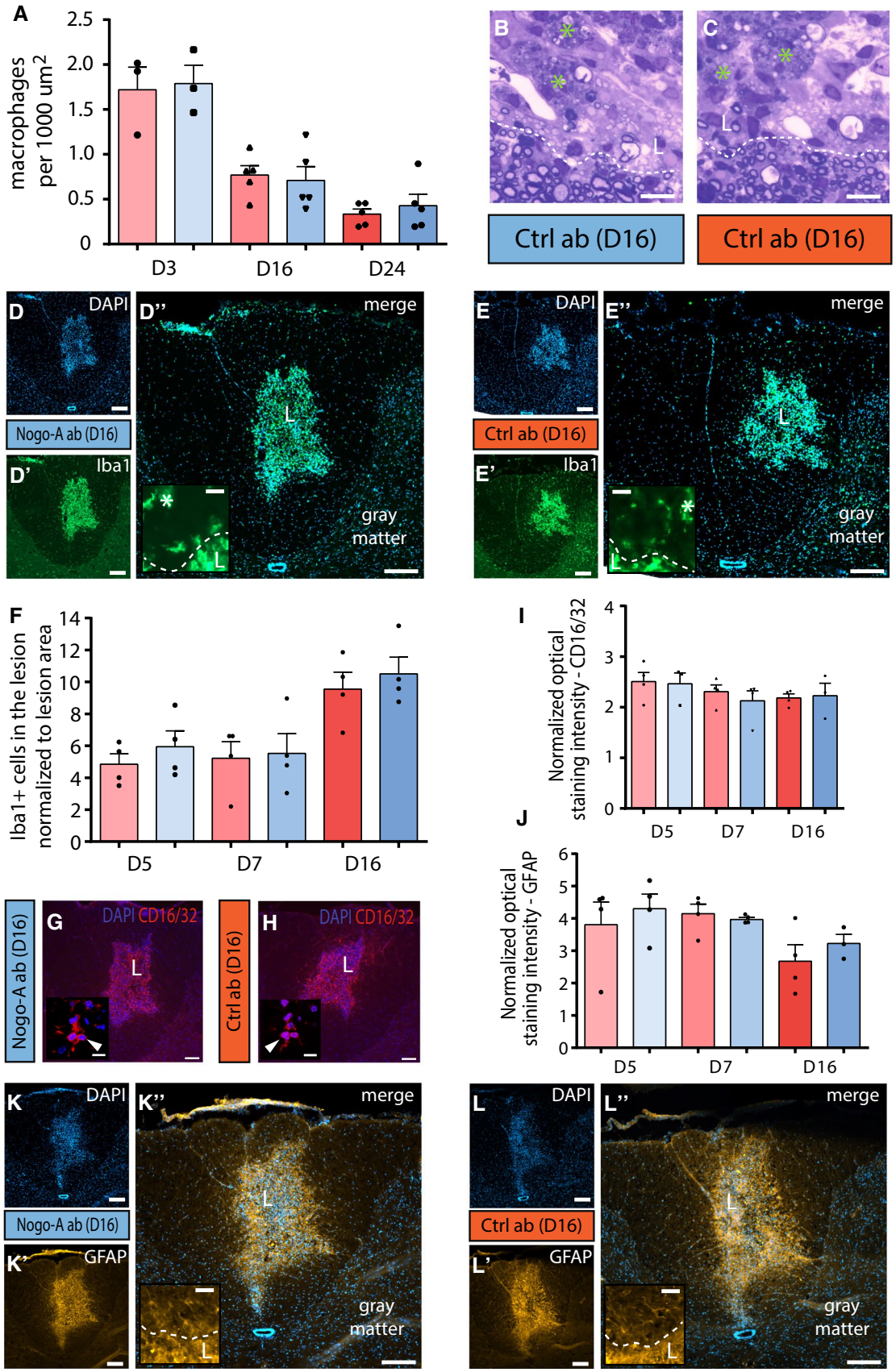
A
macrophages per 1000 um2
2.5
2.0
1.5
1.0
0.5
0
D3
D16
D24
B
C
L
Ctrl ab (D16)
Ctrl ab (D16)
D
DAPI
D''
merge
Nogo-A ab (D16)
D'
Iba1
L
gray matter
E
DAPI
E''
merge
Ctrl ab (D16)
E'
Iba1
L
gray matter
F
Iba1+ cells in the lesion normalized to lesion area
14
12
10
8
6
4
2
0
D5
D7
D16
I
Normalized optical staining intensity - CD16/32
4
3
2
1
0
D5
D7
D16
J
Normalized optical staining intensity - GFAP
6
5
4
3
2
1
0
D5
D7
D16
Nogo-A ab (D16)
G
DAPI CD16/32
L
Ctrl ab (D16)
H
DAPI CD16/32
L
K
DAPI
K''
merge
Nogo-A ab (D16)
K'
GFAP
L
gray matter
L
DAPI
L''
merge
Ctrl ab (D16)
L'
GFAP
L
gray matter

◂**Fig. 5** Reactions of microglia/macrophages and astrocytes after demyelination and upon Nogo-A-antibody treatment. There was no difference in the amount of macrophages in semithin sections at no assessed timepoint between the treatment groups (**a**–**c** macrophages defined as cells densely packed with myelin debris [25], *green asterisk* label macrophages; $n = 3$ per group at day 3 and $n = 5$ per group at days 16 and 24). Abundant signal of Iba1 immunostaining within the lysolecithin lesion at days 5, 7, and 16 suggests strong microglial and/or macrophage activation (anti-Nogo-A: **d**–**d**″, Ctrl: **e**–**e**″, white asterisk marks Iba1 + cells), with no difference in Iba + cell counts between the treatment groups (**f**, $n = 4$ per group). There is no difference in staining intensity of CD16/32 positive pro-inflammatory M1 macrophages. (**g**, **h**, and **i** quantification; inlets: white arrowheads label DAPI-CD16/32 double-positive cell). A strong astrocyte reaction in the lesion is shown by high GFAP signal with no difference between both treatment groups (anti-Nogo-A: **k**–**k**″, Ctrl: **l**–**l**″, J quantification, $n = 4$ per group). *Bars* represent mean ± SEM. Statistical analysis was done using a two-way ANOVA repeated measure followed by Bonferroni's multiple-comparison test. All immunoimages are from day 16 after lesion induction. Scalebars: **b**, **c** 20 µm, **d**–**d**″, **e**–**e**″, **g**, **h**, **k**–**k**″, and **l**–**l**″ 100 µm, all inlets 10 µm. *White dashes line* represents lysolecithin lesion border. *Ab* antibody, *Ctrl* control antibody, *L* lesion

double-positive cells (oligodendrocytes) within the lesion showed an increase of these cells over time, most likely representing the oligodendroglial repopulation of the lysolecithin lesion over time. It did, however, yield no difference between the treatment groups at neither timepoint (Fig. 6h–h″, i–i″, j). This was confirmed using MBP staining to identify mature and pre-mature oligodendrocytes within the lysolecithin lesion (Fig. 6k–m).

Together, these results show that Nogo-A neutralization using antibodies does not alter OPC proliferation, migration, or differentiation into oligodendrocytes.

Discussion

We investigated the potential therapeutic effect of anti-Nogo-A antibodies on different multiple sclerosis pathomechanisms in two animal models. First, in targeted EAE, a localized neuro-inflammatory animal model [23], anti-Nogo-A enhanced functional recovery in two fine motor skill behavioural paradigms. Whereas no underlying changes in lesion cell counts were observed, a significant increase in sprouting CST fibers entering the gray matter and arborizing preferentially to pre-motor and motor laminae was observed. Second, in lysolecithin-induced lesions, anti-Nogo-A boosted remyelination at early and later timepoints as shown by light and electron microscopy. No changes in either microglia/macrophage/astrocyte reactivity or OPC proliferation, migration, or differentiation could be observed, suggesting that myelin formation and wrapping could be the mechanisms involved in this myelin repair.

From a pathological view, multiple sclerosis is defined in its early stages by acute infiltration of immune cells into CNS tissue causing myelin destruction and, already early in the disease, primary and secondary neurodegeneration. The latter two mechanisms become more prominent during the progressive disease course, while acute and relapsing inflammation declines and develops into a chronic compartmentalized neuro-inflammation [30]. As a consequence, three therapy approaches are indicated for (progressive) multiple sclerosis: (1) dampening the inflammatory response; (2) protecting neurons and boost axonal repair for circuit reformation; and (3) salvaging intact or regenerating disintegrated myelin.

Inflammatory response upon Nogo-A neutralization

The CST is an important descending tract system from the motor cortex and critically involved in execution of fine motor movements in rodents, primates, and humans [5, 50]. Spinal multiple sclerosis lesions affecting the CST are common and are important contributors for motor dysfunction in multiple sclerosis patients [4]. To study behavioural recovery upon Nogo-A neutralization, we induced a single neuro-inflammatory lesion targeting the CST in the cervical spinal cord. At days 21 and 28 post lesion induction, anti-Nogo-A-antibody-treated rats showed enhanced functional recovery of fine motor skills. The targeted EAE lesions are defined by infiltration of macrophages, CD3+ T cells, and microglial activation with subsequent demyelination and axonal injury, thereby closely resembling multiple sclerosis lesions [23]. The peak of inflammation of these lesions is around 1 week after cytokine injection. Nogo-A neutralization could have dampened the inflammatory response thereby mediating the improved recovery. It has already been shown that T cells from Nogo-A-deficient mice show a shift towards an anti-inflammatory cytokine profile with an increase of TGF-β and IL-10, and decreased IFN-γ secretion upon EAE induction [20]. Another study revealed that adoptive transfer of Nogo-reactive T cells ameliorates EAE in mice [9]. Furthermore, NgR1, a Nogo-A receptor, has been shown to mediate the efflux of macrophages from inflamed peripheral nerves [13]. In the targeted EAE lesion paradigm, however, 3D lesion volume reconstructions and cell counts within the lesion were not altered. This indicates that the amount of inflammatory cells entering the CNS has not grossly changed upon acute, antibody-mediated Nogo-A-neutralization.

Axonal regeneration and plasticity in the spinal cord

Nogo-A neutralization, genetic ablation, or antagonization has been shown to induce enhanced sprouting and axonal regeneration in a number of studies mainly in spinal cord

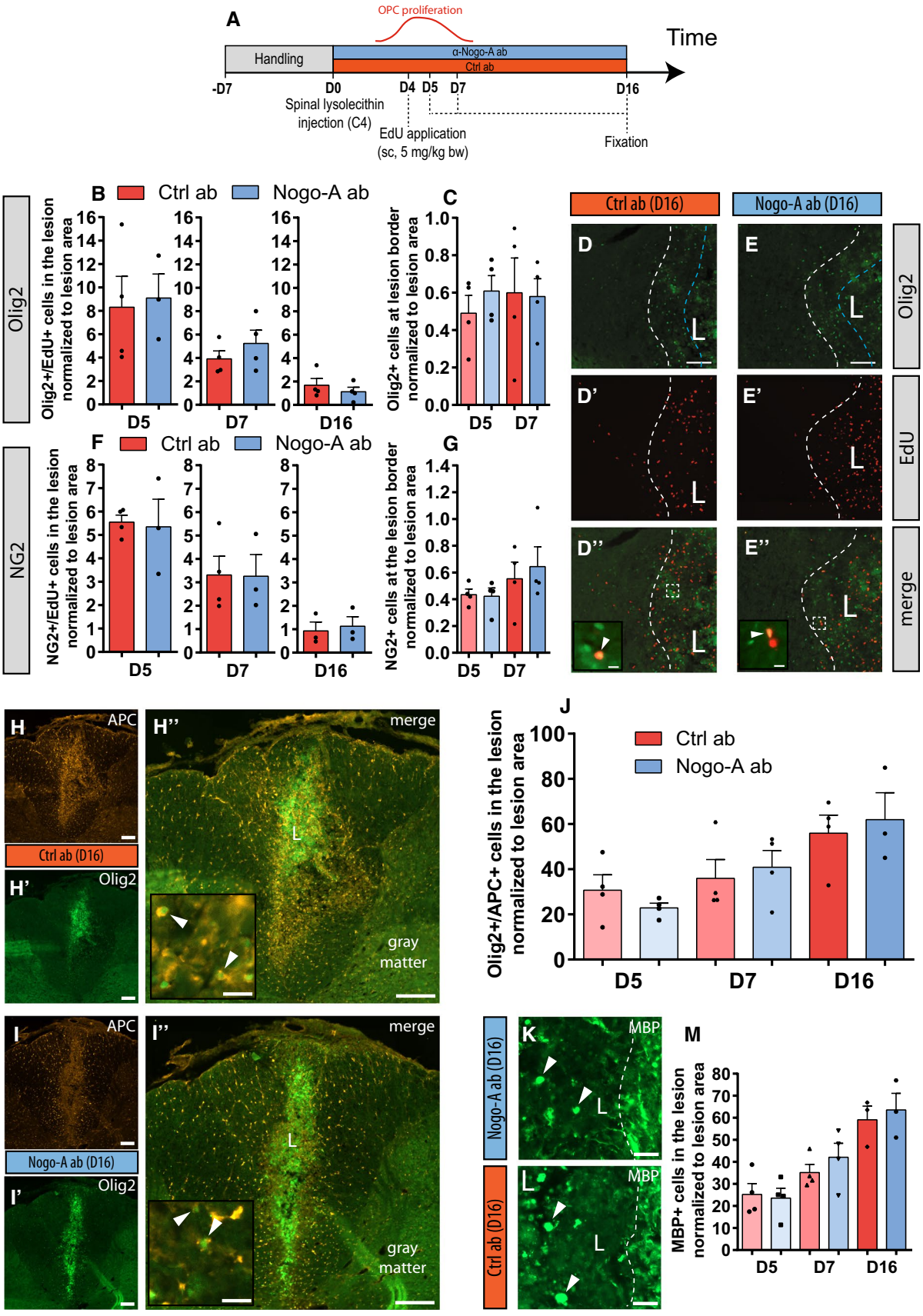
A
OPC proliferation
Time
Handling
α-Nogo-A ab
Ctrl ab
-D7
D0
D4
D5
D7
D16
Spinal lysolecithin injection (C4)
EdU application (sc, 5 mg/kg bw)
Fixation
B
Ctrl ab
Nogo-A ab
Olig2
Olig2+/EdU+ cells in the lesion normalized to lesion area
C
Olig2+ cells at lesion border normalized to lesion area
D5
D7
D16
Ctrl ab (D16)
Nogo-A ab (D16)
D
E
D'
E'
D''
E''
L
Olig2
EdU
merge
F
NG2
NG2+/EdU+ cells in the lesion normalized to lesion area
G
NG2+ cells at the lesion border normalized to lesion area
H
APC
H''
merge
Ctrl ab (D16)
H'
Olig2
gray matter
J
Olig2+/APC+ cells in the lesion normalized to lesion area
I
I''
Nogo-A ab (D16)
I'
K
MBP
M
MBP+ cells in the lesion normalized to lesion area

◂**Fig. 6** Reactions of oligodendrocyte precursor cells (OPCs) and oligodendrocytes after demyelination and upon Nogo-A-antibody treatment. **a** Experimental timeline: after induction of a lysolecithin lesion at spinal level C3 and implantation of a subcutaneous mini pump with Nogo-A- or control antibodies, rats were injected subcutaneously with 5 mg/kg bodyweight EdU at day 4 (around peak of OPC proliferation). Rats were sacrificed at days 5, 7, and 16 after lesion induction to assess OPC proliferation, migration, and differentiation. (**B**, **d**–**d**″, **e**–**e**″, *white arrowheads* label Olig2/EdU double-positive cells): Olig2/EdU double-positive cells in the lysolecithin lesion (ctrl antibody: **d**–**d**″; anti-Nogo-A: **e**–**e**″) decrease over time, probably due to dilution of the EdU label, but show no difference between treatment groups (**b**, $n = 4$ per group). **h** No difference in the amount of Olig2 positive cells at the lesion border (a 50 µm-thick concentric strip at the lesion border, shown in images **d** and **e** as area between white and blue dashed line) at days 5 and 7 between treatment groups suggests no major enhancement of OPCs to the lesion border/zone of remyelination by anti-Nogo-A treatment. **f**, **g** as well no difference in the amount of NG2/EdU double-positive cells in the lysolecithin lesion (**f**, $n = 4$ per group) or the amount of NG2 cells (OPCs) at the lesion border at earlier timepoints (**g**, $n = 4$ per group) between the treatment groups. **h**–**j** Similar amounts of Olig2/APC double-positive cells (oligodendrocytes) within the lesion between the treatment groups (Ctrl antibody: **h**–**h**″, anti-Nogo-A: **i**–**i**″, *white arrowheads* label Olig2/APC double-positive cells, J quantification, $n = 4$ per group). These data are confirmed by the counts of MBP positive cell bodies within the lesion showing no difference between the treatment groups at neither of the assessed timepoints (anti-Nogo-A: **k**, Ctrl antibody: **l**, *white arrowheads* label MBP positive cells, **m** quantification, $n = 4$ per group). All cell counts are normalized to lesion area and lesion borders (depicted as white dashed lines) are defined by DAPI counterstaining on corresponding or adjacent sections. *Bars* represent mean ± SEM. Statistical analysis was done using a two-way ANOVA repeated measure followed by Bonferroni's multiple-comparison test. All immuno-images are from day 16 after lesion induction. *Scalebars* **d**–**d**″ and **e**–**e**″ 40 µm, **h**–**h**″ and **i**–**i**″ 100 µm, all inlets as well as K and L 8 µm. *Ab* antibody, *Ctrl* control antibody, *L* lesion, *OPC* oligodendrocyte precursor cell, *sc* subcutaneous

injury and stroke animal models [48]. In EAE, Nogo-A ablation or neutralization by antibodies had neuro-protective effects [20, 41]. However, it remained unclear whether Nogo-A antibodies could boost also neuronal repair under neuro-inflammatory conditions. Therefore, we addressed the potential of Nogo-A antibodies to enhance axonal regeneration after inducing a single neuro-inflammatory lesion to the cervical spinal cord of rats. The present data show abundant growth of fibers from the descending CST at and above the neuro-inflammatory lesion upon Nogo-A-neutralization; these fibers may come from injured CST fibers and/or from unlesioned fibers which show compensatory sprouting into the gray matter. An additional neuroprotective effect of Nogo-A-neutralization cannot be ruled out completely by our data, however. These fibers seemed to preferentially target the pre-motor and motor laminae 5–8 in the gray matter 7 weeks after lesion induction, strongly indicating a directed growth rather than aberrant and unspecific fiber growth.

Kerschensteiner and colleagues were able to show that plastic neuronal changes appear on different levels upon induction of a single neuro-inflammatory lesion in the spinal cord [22]: (1) remodelling of projection neurons in the motor cortex; (2) regenerative sprouting of local interneurons surrounding the lesion, and, most importantly regarding our data; and (3) rostro-lesional CST axons extending collaterals establishing new functional circuits. The functional relevance of these anatomical "detour" circuits was further demonstrated by specific re-lesioning of the CST at brain stem level with subsequent drop in re-gained behavioural performance. Therefore, the CNS is capable to react to a neuro-inflammatory injury with specific plastic responses to restore function. In multiple sclerosis during the early relapsing stages of the disease, when neurodegeneration can already be prominent [8, 54], patients show spontaneous and complete recovery from these acute bouts. This can at least in part be explained by compensation through neuronal plasticity [52]. As soon as this repair capacity exceeds a certain limit, as the currently prevailing view suggests, the relapsing disease course converts to the progressive disease stage [30]. At this disease stage, neurodegeneration is considered to be the major cause of progressive and permanent disability [30, 53, 60]. Therefore, boosting this intrinsic neuronal capacity for self-repair, e.g., by neutralization of the growth inhibitory protein Nogo-A, is an attractive strategy for enhancing recovery during early and later stages of the disease. Thus, our data present for the first time a frame work for therapies which boost neuronal regeneration under neuro-inflammatory conditions.

Even though the data from the CST arborisation pattern indicate a directed growth towards motor layers of the spinal cord, the final functional relevance of these fibers remains to be determined. They potentially need to be consolidated, e.g., via specific training and rehabilitation as it has been shown before in a stroke animal model [55].

Enhanced remyelination

Boosting remyelination is another important approach to restore function of axons and behavioral recovery in EAE and multiple sclerosis [10]. In addition to allowing fast impulse conduction, myelin sheaths can provide critical metabolic support for axons [14]. Remyelination can, therefore, protect axons from further degeneration [19, 59]. Myelin repair is of importance for the acute and in particular for the chronic multiple sclerosis disease stage, during which lack of remyelination is a pathologic hallmark. The reasons for this failure are still unknown [12].

Our data demonstrate that Nogo-A neutralization by antibodies enhanced remyelination at early and later timepoints after experimental demyelination of the spinal cord induced by lysolecithin. Importantly, the effect seems to be mediated specifically by Nogo-A neutralization, since control antibodies directed against BrdU

or cyclosporine-A did not increase remyelination. In addition, the antibody does not interfere with the demyelination process caused by lysolecithin. This is shown by similar baseline demyelination at day 3 after lesion induction. Electron microscopy analysis of remyelination confirmed these findings.

This enhanced remyelination could either be mediated via indirect effects on the lesion-surrounding environment or via direct effects on cells of the oligodendrocyte lineage. Our data support neither of these two hypotheses: microglia/macrophage density within the lesion was unaltered as shown by different stainings. There was also no difference in the density of cytotoxic M1 macrophages within the lesions. Several studies have shown that the cytotoxic M1 macrophage is deleterious for CNS regeneration including remyelination (reviewed in [36]). This further makes any gross changes of inflammatory reaction upon Nogo-A-antibody treatment unlikely. Astrocyte density within the lesion was also unchanged suggesting no major effect of Nogo-A neutralization on astrocyte reactivity.

In our experimental setup, Nogo-A neutralization did not alter proliferative activity or migration of OPCs as well as differentiation of OPCs to oligodendrocytes. Together, these data are in line with the hypothesis proposed by Chong and colleagues: they postulate a regulatory effect of Nogo-A on oligodendrocyte–oligodendrocyte interactions (by repulsion) and node of Ranvier formation [3]. They showed that Nogo-A deficiency led to increased myelinogenic potential of oligodendrocytes represented by an increased amount of internodes formed by a single oligodendrocyte. Our data do not directly prove a regulatory effect of Nogo-A-neutralization on the myelinogenic potential of oligodendrocytes. Nevertheless, this mechanism is likely to be responsible for the enhanced remyelination with OPC proliferation, migration, or differentiation ruled out. Our data also do not support any gross effects on microglia/macrophage and astrocyte reactivity upon Nogo-A-neutralization. Therefore, the mechanism stated by Chong and colleagues seems likely for explaining the enhanced remyelination [3].

A recent study from Pourabdolhossein and colleagues demonstrated enhanced recovery of conduction latencies of visually evoked potentials (VEPs) as well as increased OPC recruitment from the neurogenic zone of the third ventricle upon NgR1 knock-down using siRNAin the optic system [42]. The increased conduction is in line with our findings showing enhanced myelin repair in the spinal cord. On the other hand, we did not see a pro-proliferative effect on OPCs upon Nogo-A-neutralization in the spinal cord. The different anatomical sites or other specific interaction partners for NgR1 besides Nogo-A could be responsible for this discrepancy in findings (reviewed in [16]).

Conclusions

Anti-Nogo-A antibodies enhanced functional recovery after induction of neuro-inflammatory lesion in the spinal cord with concomitant peri- and supralesional axonal sprouting. The antibodies also boosted spinal remyelination after experimental demyelination. Increasing remyelination and restoration of neuronal circuits is highly desirable for all stages of multiple sclerosis. The present data show that anti-Nogo-A antibodies enhance both repair processes and, therefore, are promising as a potential therapy for relapsing–remitting multiple sclerosis but in particular for chronic-progressive multiple sclerosis for which currently no reparative therapies are available.

Acknowledgements The authors thank the assistance and support of the Center for Microscopy and Image Analysis for support with the Axio Scan Slidescanner. We thank SJ. Feinberg and L. Godowsky for help with surgery.

Authors contribution BVI, MES, CB, SK, BZ, and ML contributed to the conceptual development; BVI, CB, MPS, and SK did the targeted EAE surgery, BVI, CB, and NG analyzed data from the targeted EAE experiments; BVI, PSP, NG, MSM, and JK carried out and analyzed all experiments using lysolecithin; BVI compiled figures, BVI and MES wrote the manuscript, and ML and RM provided critical input on the manuscript.

Compliance with ethical standards

Funding We are thankful for funding from the Swiss National Science Foundation (grant no. 31003A-149315-1 to MES), the Christopher and Dana Reeve Foundation (to MES), the Swiss MS Society, the Hartmann-Müller Foundation, Zurich, the Desirée-and-Niels-Yde Foundation (to BVI) and an MD-PhD fellowship of the Swiss National Science Foundation (No. 323530_151488, to BVI).

Conflict of interest MES is a founder and board member of the University of Zurich spin-off company NovaGo Therapeutics Inc. seeking at developing Nogo-A-neutralizing therapies. RM is supported by the Clinical Research Priority Project MS of the University Zurich. BVI, SK, CB, NG, PSP, MSM, JK, MPS, ML, and BZ declare no conflict of interest.

Ethical standards For all studies including animals, all applicable international, national, and/or institutional guidelines for the care and use of animals were followed. All animal procedures and protocols were approved by the Veterinary Office of the Canton of Zurich, Switzerland. This study is written in accordance with the adapted ARRIVE guidelines for reporting of studies using MS animal models [1, 24].

References

1. Amor S, Baker D (2012) Checklist for reporting and reviewing studies of experimental animal models of multiple sclerosis

and related disorders. Mult Scler Relat Disord 1:111–115. doi:10.1016/j.msard.2012.01.003
2. Blakemore WF, Franklin RJ (2008) Remyelination in experimental models of toxin-induced demyelination. Curr Top Microbiol Immunol 318:193–212
3. Chong SY, Rosenberg SS, Fancy SP, Zhao C, Shen YA, Hahn AT, McGee AW, Xu X, Zheng B, Zhang LI et al (2012) Neurite outgrowth inhibitor Nogo-A establishes spatial segregation and extent of oligodendrocyte myelination. Proc Natl Acad Sci USA 109:1299–1304. doi:10.1073/pnas.1113540109
4. Daams M, Steenwijk MD, Wattjes MP, Geurts JJ, Uitdehaag BM, Tewarie PK, Balk LJ, Pouwels PJ, Killestein J, Barkhof F (2015) Unraveling the neuroimaging predictors for motor dysfunction in long-standing multiple sclerosis. Neurology 85:248–255. doi:10.1212/wnl.0000000000001756
5. Diaz E, Morales H (2016) Spinal cord anatomy and clinical syndromes. Semin Ultrasound CT MR 37:360–371. doi:10.1053/j.sult.2016.05.002
6. Dubois-Dalcq M, Ffrench-Constant C, Franklin RJ (2005) Enhancing central nervous system remyelination in multiple sclerosis. Neuron 48:9–12. doi:10.1016/j.neuron.2005.09.004
7. Feinstein A, Freeman J, Lo AC (2015) Treatment of progressive multiple sclerosis: what works, what does not, and what is needed. Lancet Neurol 14:194–207. doi:10.1016/s1474-4422(14)70231-5
8. Ferguson B, Matyszak MK, Esiri MM, Perry VH (1997) Axonal damage in acute multiple sclerosis lesions. Brain J Neurol 120(Pt 3):393–399
9. Fontoura P, Ho PP, DeVoss J, Zheng B, Lee BJ, Kidd BA, Garren H, Sobel RA, Robinson WH, Tessier-Lavigne M et al (2004) Immunity to the extracellular domain of Nogo-A modulates experimental autoimmune encephalomyelitis. J Immunol (Baltimore, Md: 1950) 173:6981–6992
10. Franklin RJ, Ffrench-Constant C (2008) Remyelination in the CNS: from biology to therapy. Nat Rev Neurosci 9:839–855. doi:10.1038/nrn2480
11. Franklin RJ, Ffrench-Constant C, Edgar JM, Smith KJ (2012) Neuroprotection and repair in multiple sclerosis. Nat Rev Neurol 8:624–634. doi:10.1038/nrneurol.2012.200
12. Franklin RJ, Gallo V (2014) The translational biology of remyelination: past, present, and future. Glia 62:1905–1915. doi:10.1002/glia.22622
13. Fry EJ, Ho C, David S (2007) A role for Nogo receptor in macrophage clearance from injured peripheral nerve. Neuron 53:649–662. doi:10.1016/j.neuron.2007.02.009
14. Funfschilling U, Supplie LM, Mahad D, Boretius S, Saab AS, Edgar J, Brinkmann BG, Kassmann CM, Tzvetanova ID, Mobius W et al (2012) Glycolytic oligodendrocytes maintain myelin and long-term axonal integrity. Nature 485:517–521. doi:10.1038/nature11007
15. Huang JY, Wang YX, Gu WL, Fu SL, Li Y, Huang LD, Zhao Z, Hang Q, Zhu HQ, Lu PH (2012) Expression and function of myelin-associated proteins and their common receptor NgR on oligodendrocyte progenitor cells. Brain Res 1437:1–15. doi:10.1016/j.brainres.2011.12.008
16. Ineichen BV, Plattner PS, Good N, Martin R, Linnebank M, Schwab ME (2017) Nogo-A antibodies for progressive multiple sclerosis. CNS Drugs 31:187–198
17. Ineichen BV, Schnell L, Gullo M, Kaiser J, Schneider MP, Mosberger AC, Good N, Linnebank M, Schwab ME (2017) Direct, long-term intrathecal application of therapeutics to the rodent CNS. Nat Protoc 12:104–131. doi:10.1038/nprot.2016.151
18. Ineichen BV, Weinmann O, Good N, Plattner P, Wicki C, Rushing EJ, Linnebank M, Schwab ME (2016) Sudan black: a fast, easy, and non-toxic method to assess myelin repair in demyelinating diseases. Neuropathol Appl Neurobiol. doi:10.1111/nan.12373
19. Irvine KA, Blakemore WF (2008) Remyelination protects axons from demyelination-associated axon degeneration. Brain J Neurol 131:1464–1477. doi:10.1093/brain/awn080
20. Karnezis T, Mandemakers W, McQualter JL, Zheng B, Ho PP, Jordan KA, Murray BM, Barres B, Tessier-Lavigne M, Bernard CC (2004) The neurite outgrowth inhibitor Nogo A is involved in autoimmune-mediated demyelination. Nat Neurosci 7:736–744. doi:10.1038/nn1261
21. Kempf A, Tews B, Arzt ME, Weinmann O, Obermair FJ, Pernet V, Zagrebelsky M, Delekate A, Iobbi C, Zemmar A et al (2014) The sphingolipid receptor S1PR2 is a receptor for Nogo-a repressing synaptic plasticity. PLoS Biol 12:e1001763. doi:10.1371/journal.pbio.1001763
22. Kerschensteiner M, Bareyre FM, Buddeberg BS, Merkler D, Stadelmann C, Bruck W, Misgeld T, Schwab ME (2004) Remodeling of axonal connections contributes to recovery in an animal model of multiple sclerosis. J Exp Med 200:1027–1038. doi:10.1084/jem.20040452
23. Kerschensteiner M, Stadelmann C, Buddeberg BS, Merkler D, Bareyre FM, Anthony DC, Linington C, Bruck W, Schwab ME (2004) Targeting experimental autoimmune encephalomyelitis lesions to a predetermined axonal tract system allows for refined behavioral testing in an animal model of multiple sclerosis. Am J Pathol 164:1455–1469. doi:10.1016/S0002-9440(10)63232-4
24. Kilkenny C, Browne WJ, Cuthill IC, Emerson M, Altman DG (2010) Improving bioscience research reporting: the ARRIVE guidelines for reporting animal research. PLoS Biol 8:e1000412. doi:10.1371/journal.pbio.1000412
25. Kotter MR, Setzu A, Sim FJ, Van Rooijen N, Franklin RJ (2001) Macrophage depletion impairs oligodendrocyte remyelination following lysolecithin-induced demyelination. Glia 35:204–212
26. Kotter MR, Zhao C, van Rooijen N, Franklin RJ (2005) Macrophage-depletion induced impairment of experimental CNS remyelination is associated with a reduced oligodendrocyte progenitor cell response and altered growth factor expression. Neurobiol Dis 18:166–175. doi:10.1016/j.nbd.2004.09.019
27. Lee JY, Petratos S (2013) Multiple sclerosis: does Nogo play a role? Neurosci Rev J bringing Neurobiol Neurol Psychiatry 19:394–408. doi:10.1177/1073858413477207
28. Liebscher T, Schnell L, Schnell D, Scholl J, Schneider R, Gullo M, Fouad K, Mir A, Rausch M, Kindler D et al (2005) Nogo-A antibody improves regeneration and locomotion of spinal cord-injured rats. Ann Neurol 58:706–719. doi:10.1002/ana.20627
29. Ma Z, Cao Q, Zhang L, Hu J, Howard RM, Lu P, Whittemore SR, Xu XM (2009) Oligodendrocyte precursor cells differentially expressing Nogo-A but not MAG are more permissive to neurite outgrowth than mature oligodendrocytes. Exp Neurol 217:184–196. doi:10.1016/j.expneurol.2009.02.006
30. Mahad DH, Trapp BD, Lassmann H (2015) Pathological mechanisms in progressive multiple sclerosis. Lancet Neurol 14:183–193. doi:10.1016/s1474-4422(14)70256-x
31. Maier IC, Baumann K, Thallmair M, Weinmann O, Scholl J, Schwab ME (2008) Constraint-induced movement therapy in the adult rat after unilateral corticospinal tract injury. J Neurosci Off J Soc Neurosci 28:9386–9403. doi:10.1523/jneurosci.1697-08.2008
32. Mei F, Fancy SP, Shen YA, Niu J, Zhao C, Presley B, Miao E, Lee S, Mayoral SR, Redmond SA et al (2014) Micropillar arrays as a high-throughput screening platform for therapeutics in multiple sclerosis. Nat Med 20:954–960. doi:10.1038/nm.3618
33. Metz GA, Whishaw IQ (2002) Cortical and subcortical lesions impair skilled walking in the ladder rung walking test: a new task to evaluate fore- and hindlimb stepping, placing, and co-ordination. J Neurosci Methods 115:169–179

34. Mi S, Lee X, Shao Z, Thill G, Ji B, Relton J, Levesque M, Allaire N, Perrin S, Sands B et al (2004) LINGO-1 is a component of the Nogo-66 receptor/p75 signaling complex. Nat Neurosci 7:221–228
35. Mi S, Miller RH, Tang W, Lee X, Hu B, Wu W, Zhang Y, Shields CB, Zhang Y, Miklasz S et al (2009) Promotion of central nervous system remyelination by induced differentiation of oligodendrocyte precursor cells. Ann Neurol 65:304–315. doi:10.1002/ana.21581
36. Miron VE, Zehntner SP, Kuhlmann T, Ludwin SK, Owens T, Kennedy TE, Bedell BJ, Antel JP (2009) Statin therapy inhibits remyelination in the central nervous system. Am J Pathol 174:1880–1890. doi:10.2353/ajpath.2009.080947
37. Montoya CP, Campbell-Hope LJ, Pemberton KD, Dunnett SB (1991) The "staircase test": a measure of independent forelimb reaching and grasping abilities in rats. J Neurosci Methods 36:219–228
38. Oertle T, van der Haar ME, Bandtlow CE, Robeva A, Burfeind P, Buss A, Huber AB, Simonen M, Schnell L, Brosamle C et al (2003) Nogo-A inhibits neurite outgrowth and cell spreading with three discrete regions. J Neurosci Off J Soc Neurosci 23:5393–5406
39. Ontaneda D, Fox RJ, Chataway J (2015) Clinical trials in progressive multiple sclerosis: lessons learned and future perspectives. Lancet Neurol 14:208–223. doi:10.1016/s1474-4422(14)70264-9
40. Organization WH (2008) Multiple Sclerosis International Federation. Atlas: Multiple Sclerosis Resources in the World 2008. World Health Organization, Geneva, pp 13–17
41. Petratos S, Ozturk E, Azari MF, Kenny R, Lee JY, Magee KA, Harvey AR, McDonald C, Taghian K, Moussa L et al (2012) Limiting multiple sclerosis related axonopathy by blocking Nogo receptor and CRMP-2 phosphorylation. Brain J Neurol 135:1794–1818. doi:10.1093/brain/aws100
42. Pourabdolhossein F, Mozafari S, Morvan-Dubois G, Mirnajafi-Zadeh J, Lopez-Juarez A, Pierre-Simons J, Demeneix BA, Javan M (2014) Nogo receptor inhibition enhances functional recovery following lysolecithin-induced demyelination in mouse optic chiasm. PLoS ONE 9:e106378. doi:10.1371/journal.pone.0106378
43. Reindl M, Khantane S, Ehling R, Schanda K, Lutterotti A, Brinkhoff C, Oertle T, Schwab ME, Deisenhammer F, Berger T et al (2003) Serum and cerebrospinal fluid antibodies to Nogo-A in patients with multiple sclerosis and acute neurological disorders. J Neuroimmunol 145:139–147
44. Salic A, Mitchison TJ (2008) A chemical method for fast and sensitive detection of DNA synthesis in vivo. Proc Natl Acad Sci USA 105:2415–2420. doi:10.1073/pnas.0712168105
45. Sasaki M, Lankford KL, Brown RJ, Ruddle NH, Kocsis JD (2010) Focal experimental autoimmune encephalomyelitis in the Lewis rat induced by immunization with myelin oligodendrocyte glycoprotein and intraspinal injection of vascular endothelial growth factor. Glia 58:1523–1531. doi:10.1002/glia.21026
46. Satoh J, Onoue H, Arima K, Yamamura T (2005) Nogo-A and nogo receptor expression in demyelinating lesions of multiple sclerosis. J Neuropathol Exp Neurol 64:129–138
47. Schwab ME (2010) Functions of Nogo proteins and their receptors in the nervous system. Nat Rev Neurosci 11:799–811. doi:10.1038/nrn2936
48. Schwab ME, Strittmatter SM (2014) Nogo limits neural plasticity and recovery from injury. Curr Opin Neurobiol 27:53–60. doi:10.1016/j.conb.2014.02.011
49. Stadelmann C (2011) Multiple sclerosis as a neurodegenerative disease: pathology, mechanisms and therapeutic implications. Curr Opin Neurol 24:224–229. doi:10.1097/WCO.0b013e328346056f
50. Steward O, Willenberg R (2016) Rodent spinal cord injury models for studies of axon regeneration. Exp Neurol. doi:10.1016/j.expneurol.2016.06.029
51. Theotokis P, Lourbopoulos A, Touloumi O, Lagoudaki R, Kofidou E, Nousiopoulou E, Poulatsidou KN, Kesidou E, Tascos N, Spandou E et al (2012) Time course and spatial profile of Nogo-A expression in experimental autoimmune encephalomyelitis in C57BL/6 mice. J Neuropathol Exp Neurol 71:907–920. doi:10.1097/NEN.0b013e31826caebe
52. Tomassini V, d'Ambrosio A, Petsas N, Wise RG, Sbardella E, Allen M, Tona F, Fanelli F, Foster C, Carni M et al (2016) The effect of inflammation and its reduction on brain plasticity in multiple sclerosis: MRI evidence. Hum Brain Mapp 37:2431–2445. doi:10.1002/hbm.23184
53. Trapp BD, Nave KA (2008) Multiple sclerosis: an immune or neurodegenerative disorder? Annu Rev Neurosci 31:247–269. doi:10.1146/annurev.neuro.30.051606.094313
54. Trapp BD, Peterson J, Ransohoff RM, Rudick R, Mork S, Bo L (1998) Axonal transection in the lesions of multiple sclerosis. N Engl J Med 338:278–285. doi:10.1056/NEJM199801293380502
55. Wahl AS, Omlor W, Rubio JC, Chen JL, Zheng H, Schroter A, Gullo M, Weinmann O, Kobayashi K, Helmchen F et al (2014) Neuronal repair. Asynchronous therapy restores motor control by rewiring of the rat corticospinal tract after stroke. Science (New York, NY) 344:1250–1255. doi:10.1126/science.1253050
56. Weinmann O, Schnell L, Ghosh A, Montani L, Wiessner C, Wannier T, Rouiller E, Mir A, Schwab ME (2006) Intrathecally infused antibodies against Nogo-A penetrate the CNS and downregulate the endogenous neurite growth inhibitor Nogo-A. Mol Cell Neurosci 32:161–173. doi:10.1016/j.mcn.2006.03.007
57. Weinshenker BG (1998) The natural history of multiple sclerosis: update 1998. Semin Neurol 18:301–307. doi:10.1055/s-2008-1040881
58. Woodruff RH, Franklin RJ (1999) Demyelination and remyelination of the caudal cerebellar peduncle of adult rats following stereotaxic injections of lysolecithin, ethidium bromide, and complement/anti-galactocerebroside: a comparative study. Glia 25:216–228
59. Wootla B, Denic A, Watzlawik JO, Warrington AE, Rodriguez M (2015) Antibody-Mediated Oligodendrocyte Remyelination Promotes Axon Health in Progressive Demyelinating Disease
60. Wujek JR, Bjartmar C, Richer E, Ransohoff RM, Yu M, Tuohy VK, Trapp BD (2002) Axon loss in the spinal cord determines permanent neurological disability in an animal model of multiple sclerosis. J Neuropathol Exp Neurol 61:23–32
61. Yang Y, Liu Y, Wei P, Peng H, Winger R, Hussain RZ, Ben LH, Cravens PD, Gocke AR, Puttaparthi K et al (2010) Silencing Nogo-A promotes functional recovery in demyelinating disease. Ann Neurol 67:498–507. doi:10.1002/ana.21935